International Journal of Statistics and Applied Mathematics

ISSN: 2456-1452
NAAS Rating (2025): 4.49
Maths 2025; 10(8): 111-122

https://www.mathsjournal.com
Received: 25-06-2025
Accepted: 01-08-2025

Bipin C Bhatt
M. B. G. P. G. College,
Haldwani, Uttarakhand, India

Govind Pathak
Directorate of Higher Education
Haldwani, Uttarakhand, India

Corresponding Author:
Bipin C Bhatt
M. B. G. P. G. College,
Haldwani, Uttarakhand, India

Impact of melting heat transfer and thermal radiation on MHD hybrid nanofluid flow via a stretching cylinder in a porous medium

Bipin C Bhatt and Govind Pathak

DOI: https://www.doi.org/10.22271/maths.2025.v10.i8b.2132

Abstract
A study of influence of melting heat transfer along with thermal radiation on MHD hybrid nanofluid (Fe_2O_3–CuO/H_2O) flow through a stretching cylinder is carried out in the present work. The minute solid nanoparticles of Fe_2O_3 and CuO in base fluid water are used to analyze the heat transfer rate. Hybrid nano particles volume fraction used in the fluid has the range lying between 0 to 25%. The partial differential equations governing the motion of the fluid flow are reduced to ordinary differential equations by using suitable similarity transformations and non-dimensional parameters. The reduced ordinary differential equations are solved by using R-K shooting technique. The graphical illustrations of velocity and thermal fields for various values of parameters are analyzed. An increase in velocity and temperature of the fluid is observed when the concentration of hybrid nanofluid particles in the base fluid water is increased. It is observed with the results obtained that increasing values of various parameters like Reynolds number, porosity parameter, volume fraction of hybrid nanoparicle and radiation parameter enhanced the rate of heat exchange. Skin factor (surface drag force) and Nusselt number (surface heat transfer rate) get boosted with the rising values of Reynolds number.

Keywords: Hybrid nanofluid, stretching cylinder, Nusselt number, MHD flow, skin friction, heat transfer

Introduction
Many applications of manufacturing like food production, underground water transportation, solar heated, thermal insulating properties and fuel production etc. are consequences of heat transfer past a fluid flow. The outcome of the product quality in these industries depends upon the velocity gradient and the rate of heat transfer through the surface. The application of nano technology in various fields has attracted many researchers to work on it. The concept of nano fluid was firstly given by Choi [1] in 1995 and it was investigated by him that nanofluid has a higher thermal conductivity with respect to the base fluid. The proficiency of heat transfer in nanofluid has a significant impression on the size of particle and percentage of volume fraction of particle dispersed in the base fluids. Dilute solutions like water, oils and ethylene glycol form nanofluids when particles (nano-meter sized) of copper, carbon or the other material having some thermal conductivity are suspended in it.
The devices like refrigerators, nuclear reactor, cancer therapeutics require nanofluids for their better working. Nanofluids have a great importance in electronic and automobile industries. Several manufacturing exercises like biomedicine / pharmaceutical processes, fuel cells, pasteurization of food, microelectronics etc admits the applications of heat transfer. Later on Lee *et al.* [2], Choi *et al.* [3], Yoo *et al.* [4] and Hai *et al.* [5] observed that the addition of a small amount of nanoparticles in nanofluids increase the thermal conductivity of the fluid significantly. Crane [6] was the first who found the exact analytical solution of the problem dealing with the boundary layer flow through a stretching of elastic sheet moving linearly in its own plane.
The heat transfer flows under the effect of a magnetic field in presence of a porous medium play important role cross-hatching on ablative surfaces, transportation cooling of rocket boosters and combustion chambers in which film vaporization occurs.

The process of filtration and purification in chemical engineering, the underground water resource's study in agriculture engineering and the study of motion of water, oil and natural gas via oil reservoirs are the applications of flow in a porous medium. Various approach have been constructed to control the functioning of the boundary layer but the principle of MHD affect the flow of the fluid as per the requirement by making changes in the boundary layer patterns. A wide relevant works is present related to the heat transfer in fluidflow through continuously stretching rods and sheets. The boundary layer flow with natural convection in a nanofluid embedded in a porous medium is studied by Gorla and Chamkha [7]. Keeping in mind the application of flow via a porous medium Raptis and Kafoussias [8] and Kim [9] worked on MHD heat and mass transfer flow carrying in presence of porous medium. Wang and Chiu-On Ng [10] studied the effect of slip in the fluid flow due to a stretching cylinder numerically and analytically and observed that the velocity lowers greatly due to slip.

Nomenclature

f	dimensionless velocity of the fluid	C_p	specific heat at constant pressure
m	Melting parameter	C_f	skin-friction coefficient
c	Stretching rate	a	Constant numbers in velocity function
p	Pressure	B_0	magnetic field strength
Rd	Thermal radiation parameter		
Q	Heat source parameter		
T_s	Temperature of solid medium		
T_m	Melting surface temperature		
T_w	Temperature at wall		
w	Velocity in z direction		
u	Velocity in r direction		
T_∞	Ambient temperature		
T	temperature		
Re	Reynolds number		
M	Magnetic number		
Pr	Prandtl number		
Nu	Nusselt number		
k_{nf}	effective thermal conductivity of the nanofluid		
k_f	thermal conductivity of the base fluid		
k_s	thermal conductivity of the solid nano-particle		

Greek Symbol		**Subscripts**	
Λ	local permeability parameter	$1s$	Solid nanoparticle first
ρ_s	density of solid particle	$2s$	Solid nanoparticle second
σ_{nf}	electrical conductivity of nanofluid	nf	nanofluid
ϕ	non dimensional concentration	hnf	Hybrid nanofluid
θ	non dimensional temperature	f	Base fluid
μ_{nf}	effective dynamic viscosity of nanofluid	s	Solid particle
ρ_f	density of base fluid $[kgm^{-3}]$		
η	similarity variable	**Superscripts**	
υ_{nf}	kinematic viscosity of the nanofluid $[m^2s^{-1}]$	'	Derivative with respect to η
φ	nanoparticle volume fraction	"	Second derivative with respect to η
		'''	Third derivative with respect to η

The problem dealing with the fluid flow in the outer of a stretching cylinder has been studied by Wang [10] in 1988 which enables hollow tube extrusion in the external of fluid flow through it. He maintained the lowering of thickness of the hollow tube with keeping outer diameter of the tube almost stagnant and found that by doing so the solution resembles with the exact results of the Navier-Stokes. Ishak et. Al. [11] studied steady laminar flow involving

incompressible fluid bearing electrical conductivity in the outer of a stretched cylinder and obtained numerical results for MHD fluid flow and transfer of heat.

Ahmad *et al.* [12] studied the influence of heat source/sink on the nanofluid flow passing through a stretching cylinder. He observed that there is a dominant impact on local Nusselt number as solid volume fraction is increased. The impression of surface heat flux on steady laminar flow due to a stretching cylinder place in an incompressible viscous fluid is examined by Norfifah Bachok and Anuar Ishak [13]. It is observed by them that with mounting values of curvature parameter, at the surface of the cylinder heat transfer rate and surface shear stress increase. S. Mukhopadhyay [14] investigated the impact of mixed convection on heat transfer through a permeable stretching cylinder and founded that the velocity and temperature have opposite trends as permeability parameter is increased.

When metal oxides or carbon allotropes are hybridized with metallic nanoparticles of good thermal efficiency it helps in gaining better chemical and physical characteristics as a result the heat transfer rate in the base fluid is elevated. The fluid so formed is known as "hybrid nanofluid". The nanoparticles of metal oxide like CuO, MgO and Al_2O_3 etc. have poor thermal conductivity but better chemical stability. On the other hand the nanoparticles of metal such as gold, copper, silver, aluminium receive reasonable thermal efficiency and they are very reactive and unstable. The main drawback of nanofluid (mono-type /single component nanofluid) is that they possess either significant thermal efficiency or good physiochemical characteristics i.e. it does not hold all charecteristic needed for specific applications.

Recently, hybrid nanofluid have gained its remarkable attraction in various applications used for energy storage in photo electric devices, optical fibre coating, drug reduction, nuclear reactor cooling, cooling of electronic devices, coolant in machines, welding, lubrication, heat exchanger in solar collector and many more. Hybrid nanofluids are liquids in which two nano particles of different materials are dispersed into base fluid. Hybrid nanofluid causes significant enhancement in the features of heat transfer. Silver-water and titanium dioxide-water nanofluid flow through a stretching sheet was studied by Acharya *et al.* [15] and observed that Nusselt number (magnitude) falls with rising positive values of volume fraction Silver-water nanofluid.

Sureh *et al.* [16] firstly found hybrid nanofluid practically and noted that increase in volume fraction of nanoparticles results hike in viscosity as well as thermal conductivity of hybrid nanofluid. Devi and Devi [17] numerically studied the impact of hybrid nanofluid $\left(Cu - Al_2O_3 / Water\right)$ flow past a stretching surface placed in porous medium. Javad *et al.* [18] analyzed the influence of thermal radiation on MHD hybrid nanofluid flow through a stretching surface. Madhesh and Kalaiselvam [19] conducted experimental analysis on hybrid nanofluid and explored the impacts of forced convection on heat transfer coefficient, thermal characteristics and thermal conductivity. Shahirah Abu Bakar *et al.* [20] studied the impact of thermal radiation in a porous medium on hybrid nanofluid $\left(Ag - TiO_2 / H_2O\right)$ past a stretching sheet.

Melting heat transfer is associated with challenges in phase change occurring in the process of manufacturing taking place in glass treatment, laser ablation, electromagnetic crucible systems, metallic processing etc. Gorlaa *et al.* [21] analyzed the nanofluid flow through a melting surface in a porous medium and found that within the boundary layer temperature of the fluid falls as the melting parameter increases. Naganthran *et al.* [22] work involved the influence of melting heat transfer on Carreau thin hybrid nanofluid film flow through a sheet in an unsteady acceleration. They noted that without affecting the film thickness (liquid) melting heat transfer lessens the heat transfer rate. It was examined by Hayat *et al* [23] in the study of melting magneto convective nanofluid flow across a stretching sheet under viscous dissipation and Joule heating that heat transfer rate is squeezed with melting parameter.

It was explored by Soomro *et al* [24] under the study of flow MHD Sisko nanofluid via a linear stretching sheet that mounting value of melting parameter results in lowering the shear stress rate. A study of impact of thermal radiation and fluid-particle suspension along with melting heat transfer on hyperbolic tangent fluid through a stretching sheet was explored by Ganesh Kumar *et al* [25]. Hayat *et al.* [26] analyzed the comparative study of the flow of hybrid nanofluid (MWCNTs + Ag + Kerosene oil) through a stretched cylinder with nanofluid (MWCNTs + Kerosene oil) under melting heat transfer. Waqas *et al.* [27] investigated the impact of melting heat transfer on hybrid nanofluid flow along a stretched surface in porous medium.

Kaya and Ahmad [28] explores how changes in thermal conductivity and viscosity affect the flow of magneto hydrodynamic (MHD) heat transfer over a stretching or shrinking sheet. They found that an increase in the melting parameter brings results to an enhanced heat transfer rate which indicates that heat flows from the regions of lower to higher melting rates. Additionally, the fluid temperature is observed to be higher during the process of shrinking in comparison to the stretching process. Farroq *et al.* [29] explores the behaviour of heat transfer of (AA7075-AA7072/Methanol) hybrid nanofluid flow by incorporating the effects of non-uniform heat sources with the heat flux model of Cattaneo-Christovl. The outcomes found by them hold significant potential for improving in the field of thermal management occurs in aerospace applications, commonly used in aircraft engines. Additionally, their results could lead to significant improvement in efficiency of automotive cooling, enhance heating dissipation in electronic systems and encourage the development of technologies in renewable energy in concentrated solar power plants. Ramprasad *et al.* [30] examined magneto hydrodynamic (MHD) fluid flow within diverging and converging channel geometries, highlighting the role of melting heat transfer. The analysis integrates a hybrid approach, integrating numerical methods particularly the finite element Galerkin method along with artificial neural network (ANN) modelling to deal with study of the fluid dynamics and thermal behaviour throughout the different channel configurations.

Mathematical formulation

The laminar boundary layer flow of the hybrid nanofluid containing nanoparticles of CuO and Fe_2O_3 in the base fluid H_2O across the permeable stretching cylinder of radius a and with the constant surface mass transfer U_w is considered. It is assumed that there exist thermal equilibrium and no slip between the base fluid water and the nanoparticles. The coordinate system is chosen in such a way that z and r axes represent the axis and radial direction of the cylinder respectively as shown in Fig. 1.

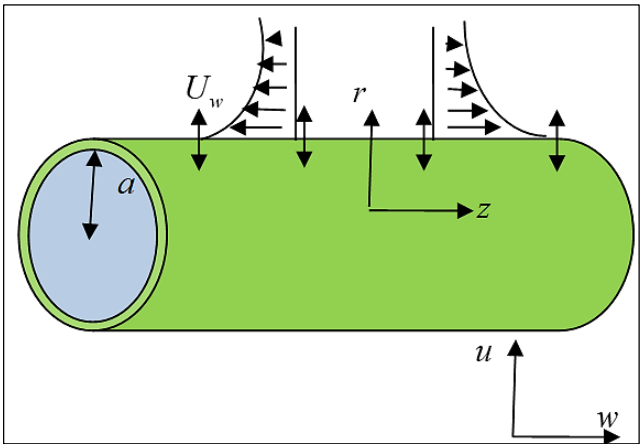

Fig 1: Coordinate system and flow configuration

The temperature of the fluid is denoted by T_w and T_l at the surface of the cylinder and at a long distance away from the cylinder respectively satisfying the condition $T_w > T_l$. Along radial direction, a uniform magnetic field B_0 is employed to the cylinder. For neglecting the impact of magnetic field induced, Magnetic Reynolds number is considered to be very small as compared to the applied uniform magnetic field. Moreover, the motion of the hybrid nanofluid is considered in a situation in which no effect of viscous dissipation, Ohmic heating and Hall Effect exists. The thermo physical properties of the hybrid nanoparticles and the base fluid are displayed in table [1]. The differential equations describing the boundary layer motion of the fluid under above specified assumptions in dimensional form are expressed as follows:

$$\frac{\partial(ru)}{\partial r}+\frac{\partial(rw)}{\partial z}=0 \tag{1}$$

$$u\frac{\partial w}{\partial r}+w\frac{\partial w}{\partial z}=\frac{\mu_{hnf}}{\rho_{hnf}}\left(\frac{\partial^2 w}{\partial r^2}+\frac{1}{r}\frac{\partial w}{\partial r}\right)-\frac{\rho_{hnf}B_0^2}{\rho_{hnf}}w-\frac{\nu_{hnf}}{K}w \tag{2}$$

$$u\frac{\partial u}{\partial r}+w\frac{\partial u}{\partial z}=-\frac{1}{\rho_{hnf}}\frac{\partial p}{\partial r}+\frac{\mu_{hnf}}{\rho_{hnf}}\left(\frac{\partial^2 u}{\partial r^2}+\frac{1}{r}\frac{\partial u}{\partial r}-\frac{u}{r^2}\right) \tag{3}$$

$$w\frac{\partial T}{\partial z}+u\frac{\partial T}{\partial r}=\frac{k_{hnf}}{\left(\rho C_p\right)_{hnf}}\left(\frac{\partial^2 T}{\partial r^2}+\frac{1}{r}\frac{\partial T}{\partial r}\right)+\frac{Q_0\left(T-T_\infty\right)}{\left(\rho C_p\right)_{hnf}}-\frac{1}{\left(\rho C_p\right)_{hnf}}\frac{\partial q_r}{\partial r} \tag{4}$$

Where q_r is given by $q_r=-\frac{4\sigma^*}{3k^*}\left(\frac{\partial T^4}{\partial r}\right)$

Subject to the boundary conditions:

$$u=0,\ w=2cz,\ T=T_w,\ k\frac{\partial T}{\partial r}=\rho\left[\lambda+C_s\left(T_m-T_0\right)\right]u \quad \text{at } r=a, \tag{5}$$

$$u\to 0,\ w\to 0,\ T\to T_\infty \quad \text{as } r\to\infty. \tag{6}$$

Here the hybrid nanofluid velocity components along the direction r and z axes are u and w respectively. The electrical conductivity, kinematic viscosity, fluid density, fluid temperature and thermal diffusivity are represented by σ,ν,ρ,T and α respectively. The stretching transpiration sheet velocities are given by $W_w=2cz$ so where c is a positive constant known as stretching rate. The physical properties of the hybrid nanofluid like, effective density ρ_{hnf}, the effective dynamic viscosity μ_{hnf}, the heat capacitance $\left(\rho C_p\right)_{hnf}$ and the thermal conductivity k_{hnf} and electrical conductivity σ_{hnf} are connected by the relations as:

$$\mu_{hnf}=\frac{\mu_f}{(1-\varphi)^{2.5}} \quad \text{where } \phi=\phi_{1s}+\phi_{2s} \tag{7}$$

$$\rho_{hnf}=(1-\phi)\rho_f+\phi_{1s}\rho_{1s}+\phi_{2s}\rho_{2s} \tag{8}$$

$$\left(\rho C_p\right)_{hnf} = (1-\phi)\left(\rho C_p\right)_f + \phi_{1s}\left(\rho C_p\right)_{1s} + \phi_{2s}\left(\rho C_p\right)_{2s} \tag{9}$$

$$k_{hnf} = \left(\frac{2(1-\phi)k_f + (1+2\phi_{1s})k_{1s} + (1+2\phi_{2s})k_{2s}}{(2+\phi)k_f + (1-\phi_1)k_{1s} + (1-\phi_2)k_{2s}}\right)k_f \tag{10}$$

$$\sigma_{hnf} = \left(1 + \frac{3\sigma_{1s}\phi_{1s} + \sigma_{2s}\phi_{2s} - \phi\sigma_f}{(1-\phi_{1s})\sigma_{1s} + (1-\phi_{2s})\sigma_{2s} + (2+\phi)\sigma_f}\right)\sigma_f \tag{11}$$

where μ_f is the dynamic viscosity of the base fluid, ϕ is the non-dimensional concentration, ρ_f and ρ_s are the densities of the water as base fluid and the nanoparticle respectively. The specific heat parameters of the first, second nanoparticles and the base fluid water are $\left(\rho C_p\right)_{1s}$, $\left(\rho C_p\right)_{2s}$ and $\left(\rho C_p\right)_f$. k_{1s}, k_{2s} and k_f are the thermal conductivities of first, second nanoparticle and the base fluid respectively. The partial differential equations governing the motion of the nanofluid are transformed into the ordinary differential equations by employing the similarity transformations as

$$u = -ca\frac{f(\eta)}{\sqrt{\eta}},\ W = 2czf'(\eta),\ \eta = \left(\frac{r}{a}\right)^2,\ \theta = \frac{T-T_\infty}{T_w-T_\infty},\ m = \frac{C_p(T_\infty - T_m)}{\lambda + C_s(T_m - T_0)} \tag{12}$$

where dash denotes differentiation with respect to η and m deals with the melting heat transfer parameter. The similarity transformations given by eq (10) reduce the governing equations (2-4) to following ordinary differential equations as:

$$\eta f''' + f'' + \frac{B}{A}.\mathrm{Re}.\left(ff'' - f'^2\right) - \frac{E}{A}BMf' - \Lambda f' = 0 \tag{13}$$

$$\left(1+\frac{Rd}{D}\right)\eta\theta'' + \frac{C}{D}\mathrm{Re}.\mathrm{Pr}.f\theta' + \frac{Q}{D}\theta + \left(1+\frac{Rd}{2D}\right)\theta' = 0 \tag{14}$$

Where the Reynolds number Re, the magnetic parameter M, porosity parameter Λ, Heat source parameter Q and thermal radiation parameter are given by $\mathrm{Re} = \frac{ca^2}{2v_f}$, $M = \frac{\sigma B_0^2 a^2}{4v_f\rho_f}$, $\Lambda = \frac{a^2}{4K}$, $Q = \frac{Q_0 a^2}{4K_f}$ and $Rd = \frac{16\sigma^* T_\infty^3}{3k^* k_f}$ respectively. Further, the constant A, B, C, D, E are taken as

$$A = \frac{1}{(1-\phi)^{2.5}},\quad B = (1-\phi) + \frac{\phi_{1s}\rho_{1s} + \phi_{2s}\rho_{1s}}{\rho_f},$$

$$C = (1-\phi) + \frac{\phi_{1s}\left(\rho C_p\right)_{1s} + \phi_{2s}\left(\rho C_p\right)_{2s}}{\rho_f},\quad D = \frac{2(1-\phi)k_f + (1+2\phi_{1s})k_{1s} + (1+2\phi_{2s})k_{2s}}{(2+\phi)k_f + (1-\phi_1)k_{1s} + (1-\phi_2)k_{2s}},$$

$$E = 1 + \frac{3\sigma_{1s}\phi_{1s} + \sigma_{2s}\phi_{2s} - \phi\sigma_f}{(1-\phi_{1s})\sigma_{1s} + (1-\phi_{2s})\sigma_{2s} + (2+\phi)\sigma_f}$$

Using the similarity transformations defined in the problem, the boundary conditions given by eq. (5) and (6) become:

$$f'(1) = 1,\ \theta(1) = 1,\ \mathrm{Pr}.f(1) + m\theta'(1) = 0 \tag{15}$$

$$f'(\infty) \to 0,\quad \theta(\infty) \to 0 \tag{16}$$

The pressure can now be determined from eq. (13) in the following form:

$$\frac{p-p_\infty}{\rho cv}=-\frac{\mathrm{Re}}{\eta}f^2(\eta)-2f'(\eta) \tag{17}$$

The skin friction coefficient and the Nusselt number are defined as follows:

$$C_f=\frac{\tau_w}{\rho W_w/2},\quad Nu=\frac{aq_w}{k(T_w-T_\infty)} \tag{18}$$

Furthermore, the skin friction τ_w and the heat transfer q_w from the surface of the cylinder are given as:

$$\tau_w=\mu\left(\frac{\partial W}{\partial r}\right)_{r=a},\quad q_w=-k\left(\frac{\partial T}{\partial r}\right)_{r=a} \tag{19}$$

where k denotes the thermal conductivity. Using the similarity transformations given by (10) in (14) and (15) we get:

$$C_f.(z\,\mathrm{Re}/a)=f''(1),\quad Nu=-2\theta'(1) \tag{20}$$

Results and Discussion

The effects of various parameters in the current problem on the fluid flow velocity, temperature, skin friction and Nusselt number have been discussed in order to deliver a good insight of the problem addressed in this study by setting numerical values to the parameters involved in the problem. For most of the results unless otherwise stated, the values of the parameters are chosen as $M=1,\ m=0.1,\ \mathrm{Pr}=7,\ Rd=0.1,\ Q=0.1,\ \Lambda=1$ .Numerical computation for $1\le \mathrm{Re}\le 5,\ 0.1\le m\le 1,\ 0.1\le Rd\le 3,\ 0.1\le Q\le 5,\ 0.1\le \phi_1\le 0.3,\ 0.1\le \phi_2\le 0.3$ and $1\le\Lambda\le 9$ has been performed to observe the influence on the flow of hybrid nanofluid through the cylinder. The velocity and temperature profiles for various values of porosity parameter Re with constant magnetic field and Prandtl number are displayed in figure [2] and figure [3] respectively. It can be noted from the figures that the impression of increase in Reynolds number Re causes decrease in both the velocity and temperature of the hybrid nanofluid flow.

Figure [4] and [5] show the behavior of upgrading values of porosity parameter Λ on velocity and thermal distribution respectively by keeping magnetic field constant. It can be observed from the figures that the greater values of Λ slow down the flow of the fluid, while temperature distribution shows an opposite trend. The influence of different values CuO and Fe_2O_3 nano particle volume fraction ϕ_1 and ϕ_2 on velocity and temperature profile is realized in figures [6] and [7]. It is inferred from the figures [6] and [7] that increasing values of ϕ_1 and ϕ_2 results hike in velocity of the fluid and thermal boundary layer. It happens because heat transfer climbs with rising values of nano particle volume fraction ϕ_1 and ϕ_2 which thus gives the impression on rise in temperature.

The impression of different values of melting parameter on the velocity distribution and temperature profile is displayed in figures [8] and [9]. The consequences of boosting the values of melting parameter appearing in these figures show that within the boundary layer there is a decrease in both the velocity and temperature distribution. The consequences of heat source sink parameter and thermal radiation on temperature profile of the fluid flow is layout in figures [10] and [11] respectively. These figures realize that the temperature of the fluid declines away from the surface of the cylinder and becomes zero far away from the cylinder for a particular value of Q and Rd . It can be perceived also from the figures [10] and [11] that there is an upsurge in the temperature of fluid for growing values of Q and Rd .

The figure [12] set forth the variation of Reynolds number Re and porosity parameter Λ on $f''(1)$ (skin factor or surface drag force). Surface drag force get elevated monotonically with applying increments Re and Λ. The surface heat transfer rate (or Nusselts number) $-\theta'(1)$ is displayed in figure [13] for different Re and Λ. It is observed from this figure that Nusselts number shows uplift when Reynolds number values are mounted and a contradictory pattern is noted with rising values of porosity parameter. Table [3] presents the comparison of current results with the outcomes found by the researchers in past studies and it can be concluded from this comparison that the current results resembles with them.

Table1: Thermo-Physical properties of hybrid nanofluid containing water and nanoparticles:

Thermophysical Properties	Fe_2O_3 **taken as first nanoparticle** (ϕ_1)	CuO **taken as second nanoparticle** (ϕ_2)	**Base Fluid** H_2O
$\rho(kg/m^3)$	3970	6500	997.1
$C_p\ (J/Kg.K)$	765	531.8	4179
$k(W/mK)$	40	0.85	0.613
$\sigma(1/\Omega.m)$	3.5×10^7	5.96×10^7	0.05

Table2 Values of $f''(1)$ and $-\theta'(1)$ for giving distinct values to m, Λ, Re and Q.

$\phi_1 = \phi_2$	Rd	Q	m	Re	Λ	$f''(1)$	$-\theta'(1)$
0.1	0.1	0.1	0.1	1	1	-2.06667	2.6823
0.1	0.1	0.1	0.1	1	5	-2.9599	2.5752
0.1	0.1	0.1	0.1	1	9	-3.62199	2.5028
0.1	0.1	0.1	0.1	2	1	-2.36376	3.5485
0.1	0.1	0.1	0.1	4	1	-2.91644	5.16674
0.1	0.1	0.1	0.1	5	1	-3.18855	6.0352
0.2	0.1	0.1	0.1	1	1	-1.92169	2.455
0.3	0.1	0.1	0.1	1	1	-1.64277	2.2859
0.1	0.1	0.1	0.7	1	1	-2.29254	4.4496
0.1	0.1	0.1	1.0	1	1	-2.62457	6.901
0.1	0.1	2	0.1	1	1	-2.06374	2.2953
0.1	0.1	5	0.1	1	1	-2.05748	1.4673
0.1	1	0.1	0.1	1	1	-2.06232	2.1084
0.1	3	0.1	0.1	1	1	-2.05875	1.6361

Table 3: Comparison of $f''(1)$ with miscellaneous values of Re observed for regular fluid.

Re	**Wang [10]**	**Ishak et. Al. [11]**	**Present Results**
1	-1.1781	-1.17776	-1.19222
2	-1.5941	-1.59390	-1.59947
5	-2.4175	-2.41745	-2.41853
10	-3.3445	-3.34445	-3.34465

Figures for hybrid nanofluid flow

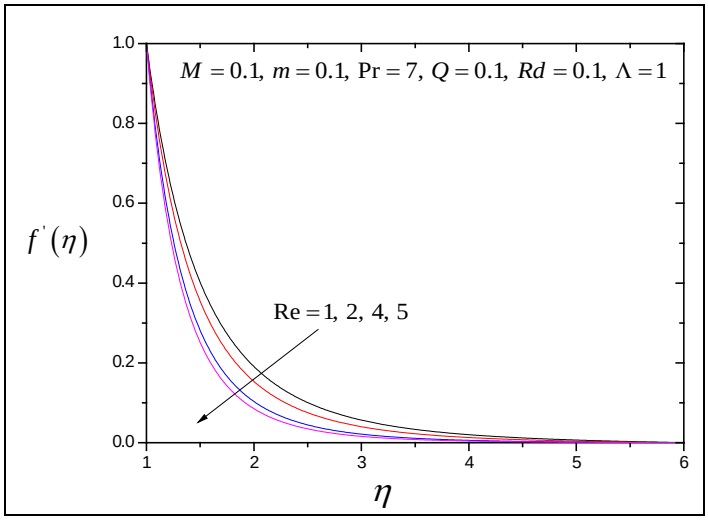

Fig 2: Velocity curve for different values of Re.

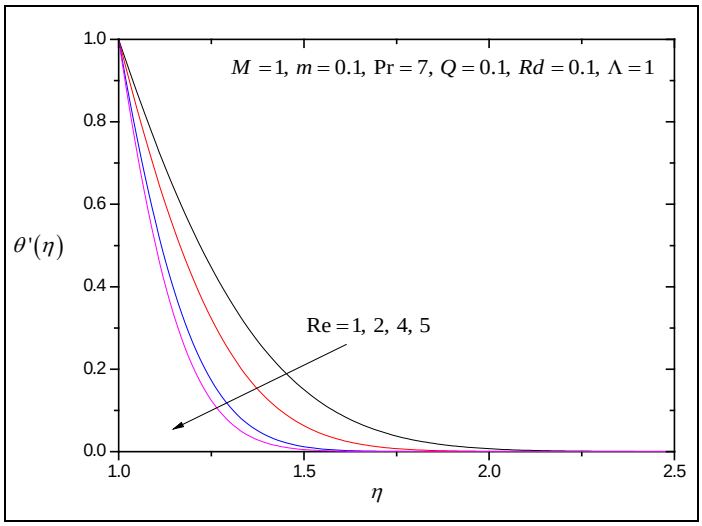

Fig 3: Temperature curve for different values of Re.

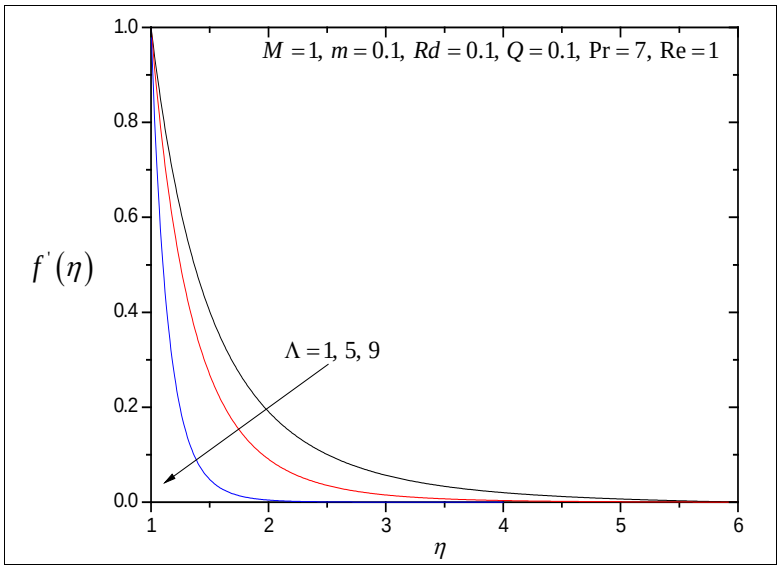

Fig 4: Velocity curve for different values of Λ.

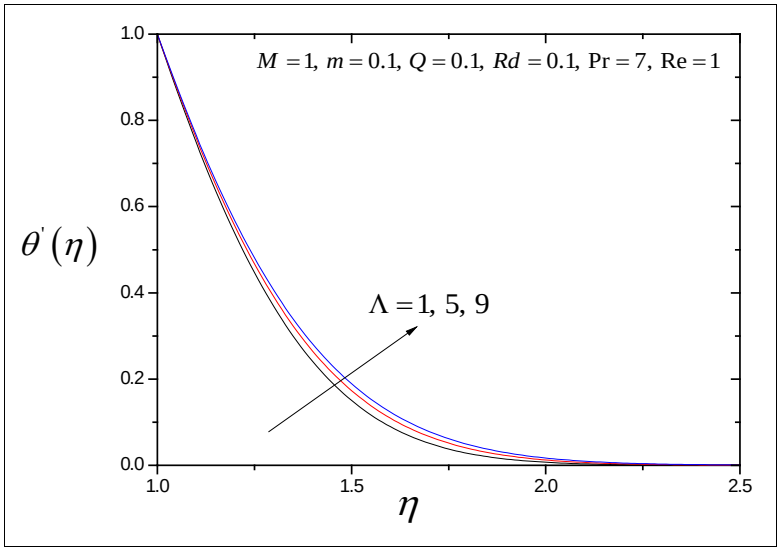

Fig 5: Temperature curve for different values of Λ.

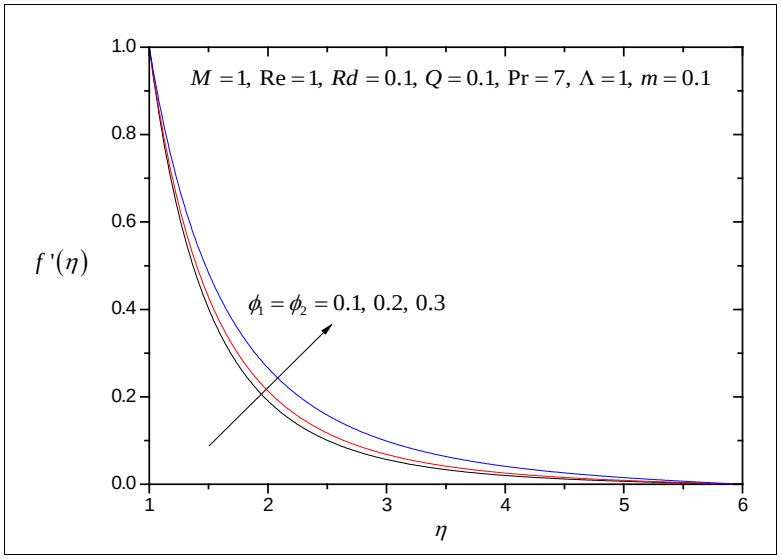

Fig 6: Velocity profile for different values of ϕ_1 and ϕ_2.

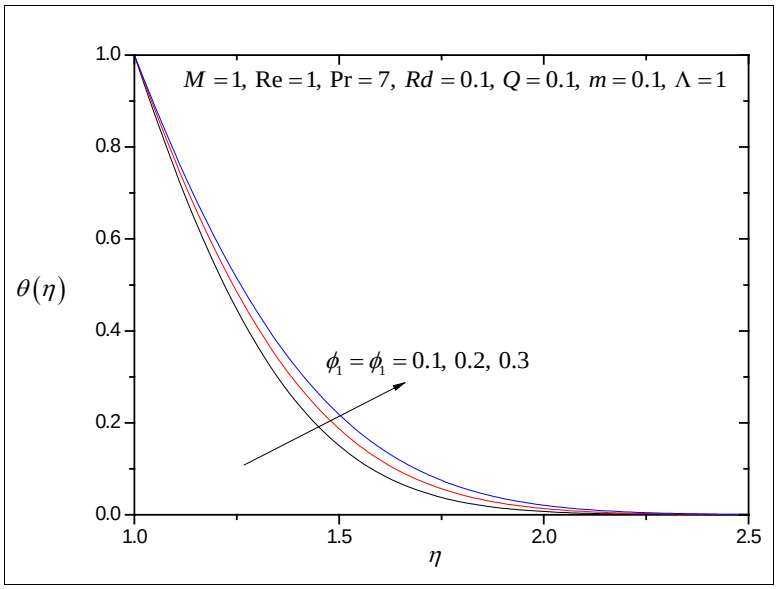

Fig 7: Temperature curve for different values of ϕ_1 and ϕ_2.

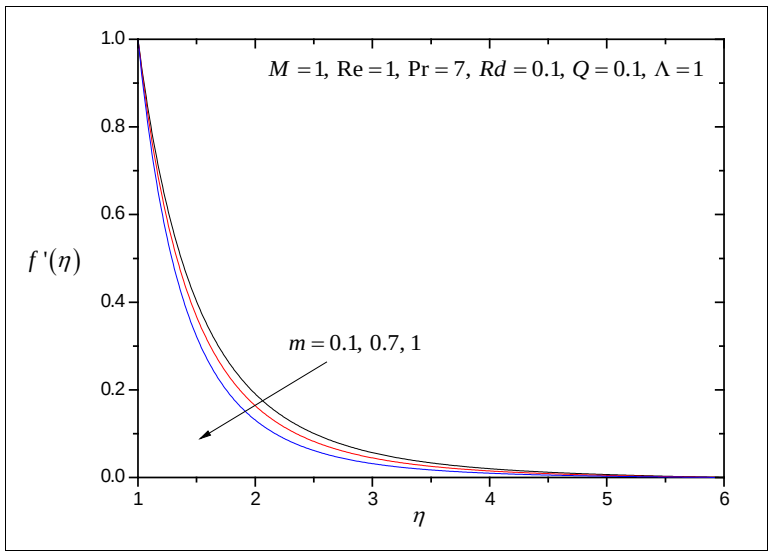

Fig 8: Velocity curve for different values of m.

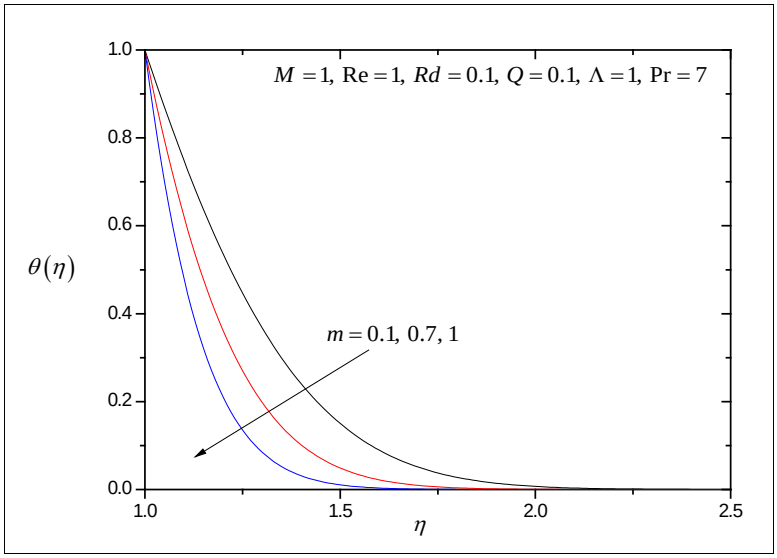

Fig 9: Temperature curve for different values of m.

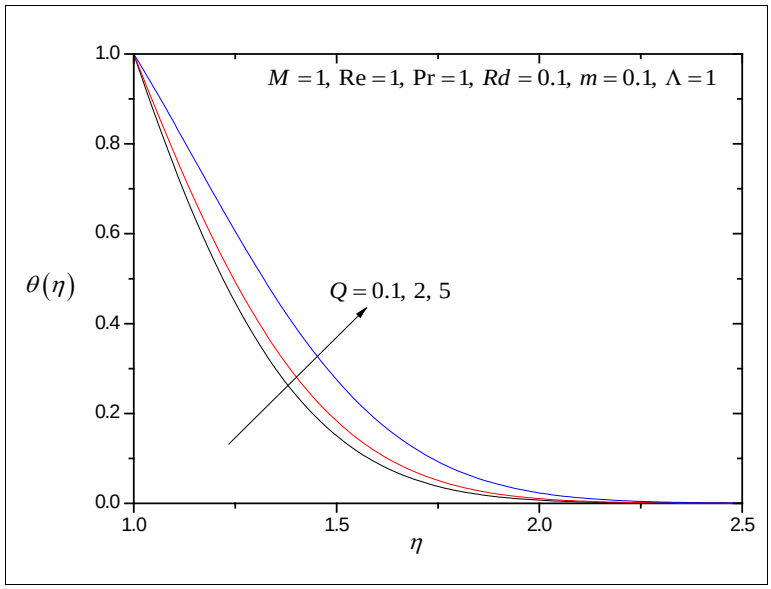

Fig 10: Temperature curve for different values of Q.

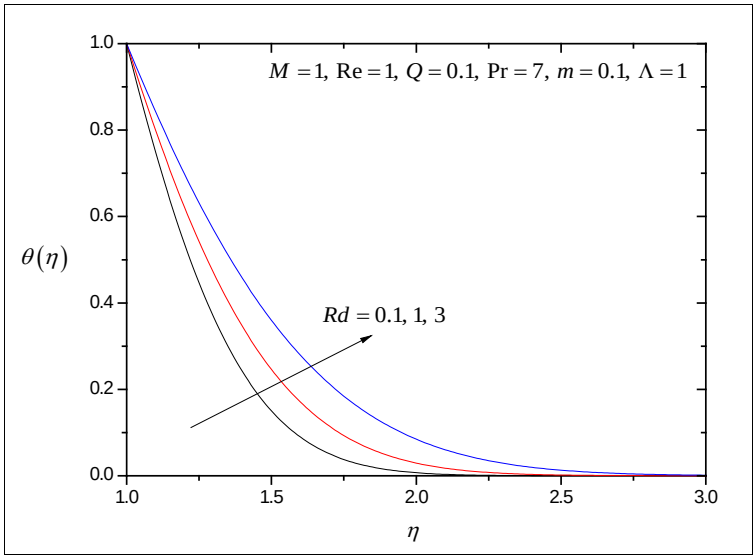

Fig 11: Temperature curve for different values of Rd.

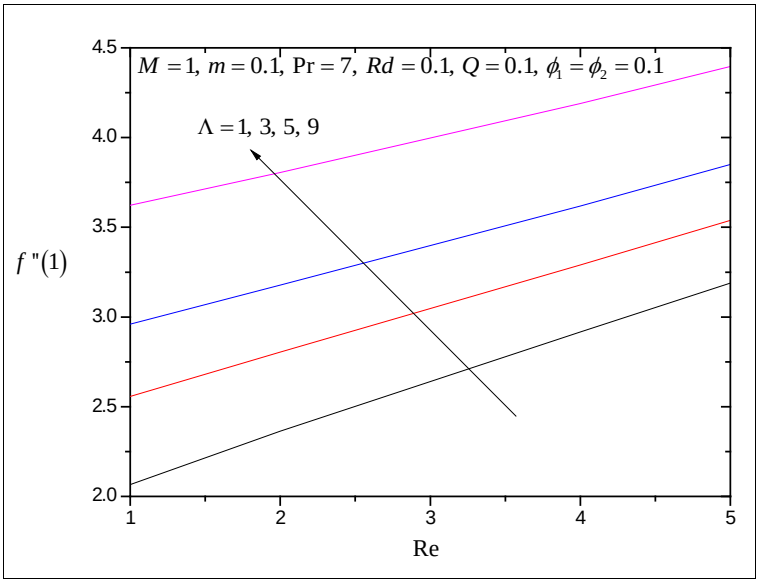

Fig 12: $f''(1)$ for different values of Re and Λ.

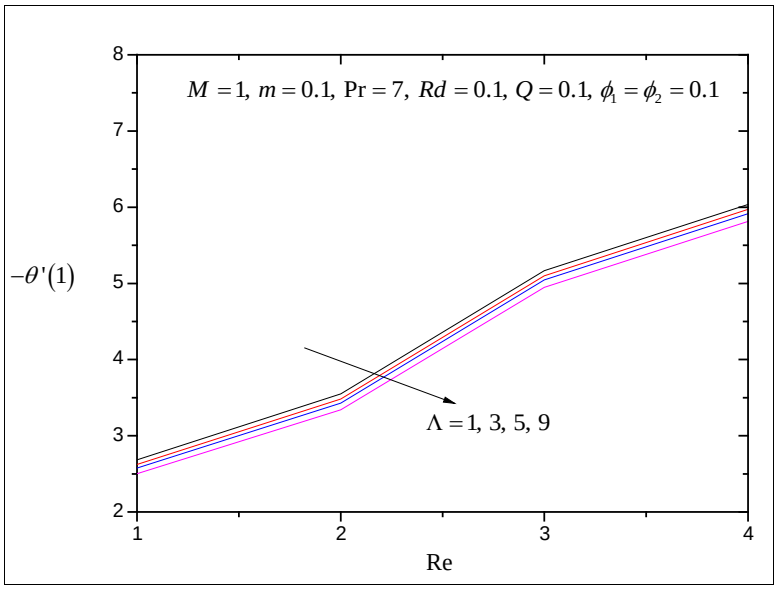

Fig 13: $-\theta'(1)$ for different values of Re and Λ.

Conclusions

Melting heat transfer impression on hybrid nanofluid flow consisting and nanoparticles through a stretching cylinder placing in porous medium is considered in this paper. The model structure defining the motion of fluid by partial differential equations along with suitable boundary conditions is transformed to ordinary differential equations by imposing similarity transformations. The transformed ODEs including boundary conditions are numerically solved by using software MATLAB and shooting technique. Graphical representation of various physical quantities has been drawn to get detailed information about the problem entertained. For controlled parameters with realistic values, it is noted that there is a decline in velocity of the fluid with growing values of various parameters such as Reynolds number, porosity parameter and melting heat parameter.

It can be seen from table [2] and various graphs drawn between temperature and varying parameters used in the problem that the temperature is magnified with heat source parameter, radiation parameter, porosity parameter, and volume fraction of nanoparticles. It is observed that for high temperature involvement nanoparticle concentration of both the nanomaterial has a significant role. From this point of view it may be banked on that this investigation may be favorable in refrigeration systems, cooling systems in air conditioning, automobile devices, electronic devices and nuclear device.

References

1. Choi SUS. Enhancing thermal conductivity of fluids with nanoparticle. ASME FED. 1995;231:99-105.
2. Lee S, Choi US, Li S, Eastman JA. Measuring thermal conductivity of fluids containing oxide nanoparticles. J Heat Transf. 1999;121:280-9.
3. Choi EJ, Ahn Y, Her YD. Size dependence of magnetic properties of *Co*-ferrite nanoparticles. J Korean Phys Soc. 2007;50:460-3.
4. Yoo DH, Hong KS, Hong TE, Eastman JA, Yang HS. Thermal conductivity of Al_2O_3/water nanofluids. J Korean Phys Soc. 2007;51:584-7.
5. Hai NH, Phu ND, Lung NH, Chau N, Chinh HD, Hoang LH, *et al*. Mechanism for sustainable magnetic nanoparticles under ambient conditions. J Korean Phys Soc. 2008;52:1327-31.
6. Crane LJ. Flow past a stretching plate. Z Angew Math Phys. 1970;21(4):645-7.
7. Gorla RSR, Chamkha A. Natural convective boundary layer flow over a horizontal plate embedded in a porous medium saturated with a nanofluid. J Mod Phys. 2011;2:62-71.
8. Raptis A, Kafoussias NG. Magnetohydromagnetic free convection flow and mass transfer through porous medium bounded by a vertical porous plate with constant heat flux. Can J Phys. 1982;60(12):1725-9.
9. Kim YJ. Heat and mass transfer in MHD micropolar flow over a vertical moving porous plate in a porous medium. Transp Porous Media. 2004;56(1):17-37.
10. Wang CY. Fluid flow due to a stretching cylinder. Phys Fluids. 1988;31(3):466-8.
11. Ishak A, Nazar R, Pop I. Magnetohydrodynamic (MHD) flow and heat transfer due to a stretching cylinder. Energy Convers Manag. 2008;49:3265-9.
12. Ahmed SE, Hussein AK, Mohammed HA, Sivasankar S. Boundary layer flow and heat transfer due to permeable stretching tube in the presence of heat source/sink utilizing nanofluids. Appl Math Comput. 2014;238:149-62.
13. Bachok N, Ishak A. Flow and heat transfer over a stretching cylinder with prescribed surface heat flux. Malays J Math Sci. 2010;4(2):159-69.
14. Mukhopadhyay S. Mixed convection boundary layer flow along a stretching cylinder in porous medium. J Pet Sci Eng. 2012;96-97:73-8.
15. Acharya N, Das K, Kundu PK. Ramification of variable thickness on MHD TiO_2 and *Ag* nanofluid flow over a slendering stretching sheet using NDM. Eur Phys J Plus. 2016;131:303.
16. Suresh S, Venkitaraj KP, Selvakumar P, Chandrasekhar M. Synthesis of Al_2O_3-Cu/water hybrid nanofluids using two-step method and its thermophysical properties. Colloids Surf A. 2011;388(1-3):41-8.
17. Devi SP, Devi SSU. Numerical investigation of hydromagnetic hybrid Cu-Al_2O_3/water nanofluid flow over a permeable stretching sheet with suction. Int J Nonlinear Sci Numer Simul. 2016;17(5):249-57.

18. Javed M, Khan Z, Bonyah E, Jan R. Analysis of hybrid nanofluid stagnation point flow over a stretching surface with melting heat transfer. Math Probl Eng. 2012;2012:1-17.
19. Madhesh D, Kalaiselvam S. Experimental analysis of hybrid nanofluid as a coolant. Procedia Eng. 2014;94:1667-75.
20. Bakar SA, Arifin NM, Bachok N, Ali FM. Effect of thermal radiation and MHD on hybrid *Ag-TiO₂*/H₂O nanofluid past a permeable porous medium with heat generation. Case Stud Therm Eng. 2021;28:101681.
21. Gorla RSR, Chamkha A, Aloraier A. Melting heat transfer in a nanofluid flow past a permeable continuous moving surface. J Nav Archit Mar Eng. 2011;8(2):83-92. doi:10.3329/jname.v8i2.6830.
22. Naganthran K, Nazar R, Siri Z, Hashim I. Entropy analysis and melting heat transfer in the Carreau thin hybrid nanofluid film flow. Mathematics. 2021;9(21):3092.
23. Hayat T, Muhammad K, Alsaedi A. Melting effect in MHD stagnation point flow of Jeffrey nanomaterial. Phys Scr. 2019;94(11):115205. doi:10.1088/1402-4896/ab210e.
24. Soomro FA, Usman M, UlHaq R, Wang W. Melting heat transfer analysis of Sisko fluid over a moving surface with nonlinear thermal radiation via collocation method. Int J Heat Mass Transf. 2018;126:1034-42.
25. Ganesh KK, Gireesha BJ, Rudraswamy NG, Gorla RSR. Melting heat transfer of hyperbolic tangent fluid over a stretching sheet with fluid particle suspension and thermal radiation. Commun Numer Anal. 2017;2:125-40.
26. Hayat T, Muhammad K, Alsaedi A. Numerical study of melting heat transfer in stagnation-point flow of hybrid nanomaterial (*MWCNTs* + *Ag* + kerosene oil). Int J Numer Methods Heat Fluid Flow. 2021;31:2580-98.
27. Waqas H, Bukhari FF, Farooq U, Alqarni MS, Muhammad T. Numerical computation of melting heat transfer in nonlinear radiative flow of hybrid nanofluids due to permeable stretching curved surface. Case Stud Therm Eng. 2021;27:101348. doi:10.1016/j.csite.2021.101348.
28. Kaye R, Ahmad S. Melting heat transfer and variable viscosity of a hydromagnetic flow over a stretching/shrinking sheet: numerical approach. JP J Heat Mass Transf. 2024;37:185-99.
29. Farroq U, Liu H, Basem A, Fatima N, Alhushavbari A, Imran M, *et al*. Computational investigation of methanol-based hybrid nanofluid flow over a stretching cylinder with Cattaneo-Christov heat flux. J Comput Des Eng. 2024;11(4):73-82. doi:10.1093/jcde/qwae059.
30. Ramprasad S, Mallikarjuna B, Pulla N. Boundary layer convective flow in a divergent channel with melting heat transfer and mass suction/injection: an analysis using ANN and numerical methods. Heat Transf. 2025;54:3405-17. doi:10.1002/htj.23363.